Available online at www.sciencedirect.com
SCIENCE DIRECT®
ELSEVIER
International Journal of Solids and Structures 43 (2006) 1818–1831
INTERNATIONAL JOURNAL OF SOLIDS and STRUCTURES
www.elsevier.com/locate/ijsolstr

Stress concentration at an elliptic hole in transversely isotropic piezoelectric solids

Longchao Dai, Wanlin Guo *, X. Wang

Institute of Nano Science, Nanjing University of Aeronautics and Astronautics, Nanjing 210016, China

Received 6 December 2004; received in revised form 26 May 2005
Available online 20 July 2005

Abstract

Two-dimensional electroelastic analyses have been performed theoretically on a transversely isotropic piezoelectric material containing an elliptic hole, subjected to a uniform stress field and a uniform electric displacement field at infinity while the surface of the hole is free of traction and electrically open. Solutions are obtained by using the exact electric boundary condition based on the complex variation method. Explicit solutions for the distributions of the mechanical and electrical components on the rim of the elliptic hole are obtained. An interesting relationship between the stress concentration factor of an elliptic hole (K_t) and that of a circular hole ($K_t|_{t=1}$), $K_t = 1 + \frac{K_t|_{t=1}-1}{t}$, is found in both elastic and piezoelectric materials. It is shown that the electromechanical coupling effect is helpful to reduce the stress concentration. And the influence of the dielectric parameter of the medium inside the hole on the stresses and the concerned stress concentration factor at the surface of the hole is weak in a wide range of the dielectric parameter. Comparisons with available results show good coincidence.

Keywords: Elliptical hole; Transversely isotropic piezoelectric; Stress concentration; Complex variation method; Electric boundary condition

1. Introduction

In recent years, the potential applications of piezoelectric materials have drawn a lot of attentions in many fields for their electromechanic-coupling effect. The main disadvantage, however, is their brittleness. Piezoelectric materials have a tendency to develop critical crack growth due to stress concentrations induced by both mechanical and electrical loads. Yet, defects are not limited to cracks. Voids, inclusions, delaminations and porosities may also exist and contribute to failures of the materials.

* Corresponding author. Tel./fax: +86 25 84895827.
E-mail address: wlguo@nuaa.edu.cn (W. Guo).

0020-7683/$ - see front matter © 2005 Elsevier Ltd. All rights reserved.
doi:10.1016/j.ijsolstr.2005.05.035

Due to the simplicity and importance, crack problems have received considerable interests for more than two decades. In 1980, Deeg analyzed dislocation, crack and inclusion problems in piezoelectric solids. To simplify the mathematical evaluation, Deeg proposed that the normal components of the electric displacement could be treated as zero at the upper and lower crack surfaces. In order to prove the validity of Deeg's approximation, Pak (1990) gave a detailed argument for neglecting the electric displacement within the crack. Sosa and Pak (1990) investigated a more general crack tip field using an eigenfunction analysis. Pak (1992); Sosa (1992) and Suo et al. (1992) analyzed the stress and electric fields near a crack. Researches on crack problems in piezoelectricity have also been conducted by Hao and Shen (1994), Zhang and Tong (1996), and Wang and Shen (2002).

The problem of a piezoelectric material containing an elliptic hole or inclusion is another important issue for its importance in both theory and applications. Sosa (1991) solved the plane strain problem for a transversely isotropic piezoelectric material containing an elliptic hole with impermeable electric boundary condition by using the theory of complex variables. Later, Sosa and Khutoryansky (1996) used the series expansion method to address the same problem but with permeable electric boundary conditions. Their results showed that the electric displacement inside the hole is constant when uniform mechanical and electric loads are applied at infinity. Gao and Fan (1999) gave an explicit, closed-form solution satisfying the exact electric boundary condition on the hole surface for the same problem. They also analyzed the stress intensity factors when the elliptic hole degenerated into a crack. Ting and Yan (1991) and Chung and Ting (1996) analyzed the plane problem for an anisotropic piezoelectric plate with either an elliptic hole or an elliptic rigid inclusion by using the Stroh formalism. Analysis on an elliptical cylinder cavity or a crack inside an infinite piezoelectric medium was performed by Zhang et al. (1998) based on the Stroh formalism and the finite element method. Recently, Deng and Wang (2002); Dai and Guo (2004); Zhou and Wang (2004) and Wang et al. (2004) found that some numerical data given by Sosa (1991) were wrong although the theoretical solutions themselves were correct.

To the best knowledge of the authors, however, there are few works that make clear the stress concentration at an elliptic hole. Based on the works of Sosa (1991), Sosa and Khutoryansky (1996), and Gao and Fan (1999), the stress concentration in a two-dimensional transversely isotropic piezoelectric plate containing an elliptic hole is completely studied in this paper. Furthermore, distributions of the mechanical and electrical components on the rim of the hole or along the x-axis are given for two different load conditions. For the case of the far field uni-axial mechanical loading, the solution of the normalized tangential stress is obtained. An interesting relationship between the stress concentration factor of a semi-elliptic hole and that of a circular hole is obtained. Using this expression, the influence of the dielectric parameter of the medium inside the hole on stress distributions and on stress concentrations is readily observed. It is found that this influence is very weak in a wide range of the dielectric parameter, but the electromechanical coupling effect is helpful to reduce the stress concentration. Some curves are given under either the far field mechanical loads or far field electric displacement loads, respectively.

2. Basic formulations of the problem

In a Cartesian coordinate system (x_1, x_2, x_3), the general equations governing the three-dimensional piezoelectricity in the absence of body forces and free charges can be written as

$$\varepsilon_{ij} = s_{ijkl}\sigma_{kl} + g_{kij}D_k, \quad E_i = -g_{ikl}\sigma_{kl} + \beta_{ik}D_k, \tag{1}$$

$$\sigma_{ij,j} = 0, \quad D_{i,i} = 0, \tag{2}$$

$$\varepsilon_{ij} = \tfrac{1}{2}(u_{j,i} + u_{i,j}), \quad E_i = -\phi_{,i}, \tag{3}$$

where $i, j, k, l = 1, 2, 3$; σ_{ij}, ε_{ij}, u_i, D_i, E_i are the components of stress, strain, displacement, electric displacement and electric field, respectively; s_{ijkl} is the compliance tensor of the material measured at zero electric displacement; g_{kij} is the piezoelectric tensor, and β_{ik} is the dielectric impermeability tensor measured at zero

stress, ϕ is the electric potential. A comma before a subscript stands for differentiation and repeated indices imply summation.

Here the Cartesian coordinates x, y, z are the principal axes of the material while the z-axis is oriented in the poling direction of the piezoelectric ceramic and the x–y plane is isotropic. We consider a transversely isotropic piezoelectric plate containing an elliptic hole with semi-axes of a and b under far field loadings. For simplicity, the following expressions are adopted:

Displacement: $u_x = u(x,z), \quad u_y = v(x,z), \quad u_z = w(x,z);$

Electric potential: $\phi = \phi(x,z).$

Following Sosa (1991), replace x, z, y with x_1, x_2, x_3 . One has

$$\begin{pmatrix} \varepsilon_{11} \\ \varepsilon_{22} \\ 2\varepsilon_{23} \\ 2\varepsilon_{12} \\ 2\varepsilon_{13} \end{pmatrix} = \begin{pmatrix} a_{11} & a_{12} & 0 & 0 & 0 \\ a_{12} & a_{22} & 0 & 0 & 0 \\ 0 & 0 & a_{33} & 0 & 0 \\ 0 & 0 & 0 & a_{44} & 0 \\ 0 & 0 & 0 & 0 & a_{55} \end{pmatrix} \begin{pmatrix} \sigma_{11} \\ \sigma_{22} \\ \sigma_{23} \\ \sigma_{12} \\ \sigma_{13} \end{pmatrix} + \begin{pmatrix} 0 & b_{12} \\ 0 & b_{22} \\ 0 & 0 \\ b_{41} & 0 \\ 0 & 0 \end{pmatrix} \begin{pmatrix} D_1 \\ D_2 \end{pmatrix}, \tag{4}$$

$$\begin{pmatrix} E_1 \\ E_2 \end{pmatrix} = -\begin{pmatrix} 0 & 0 & 0 & b_{41} & 0 \\ b_{12} & b_{22} & 0 & 0 & 0 \end{pmatrix} \begin{pmatrix} \sigma_{11} \\ \sigma_{22} \\ \sigma_{23} \\ \sigma_{12} \\ \sigma_{13} \end{pmatrix} + \begin{pmatrix} c_{11} & 0 \\ 0 & c_{22} \end{pmatrix} \begin{pmatrix} D_1 \\ D_2 \end{pmatrix}, \tag{5}$$

where

$$a_{11} = s_{11} - \frac{s_{12}^2}{s_{11}}, \quad a_{12} = s_{13} - \frac{s_{12}s_{13}}{s_{11}}, \quad a_{22} = s_{33} - \frac{s_{13}^2}{s_{11}}, \quad a_{33} = s_{44} + \frac{g_{15}^2}{\beta_{11}},$$
$$a_{44} = s_{44}, \quad a_{55} = 2(s_{11} - s_{12}), \quad b_{12} = g_{31} - \frac{s_{12}g_{31}}{s_{11}},$$
$$b_{22} = g_{33} - \frac{s_{13}g_{31}}{s_{11}}, \quad b_{41} = g_{15}, \quad c_{11} = \beta_{11}, \quad c_{22} = \beta_{33} + \frac{g_{31}^2}{s_{11}}.$$

Let $z_k = x_1 + \mu_k x_2$. Thus, expressions of all physical quantities in the x_1–x_2 plane can be expressed as follows:

$$\begin{aligned}
&\langle \sigma_{11}, \sigma_{22}, \sigma_{12} \rangle = 2\mathrm{Re} \sum_{k=1}^{3} \langle \mu_k^2, 1, -\mu_k \rangle \varphi_k'(z_k), \\
&\langle \sigma_{13}, \sigma_{23} \rangle = 2\mathrm{Re} \langle -\mu_4, 1 \rangle \varphi_4'(z_4), \\
&\langle D_1, D_2 \rangle = 2\mathrm{Re} \sum_{k=1}^{3} \langle -\lambda_k \mu_k, \lambda_k \rangle \varphi_k'(z_k), \\
&\langle E_1, E_2 \rangle = -2\mathrm{Re} \sum_{k=1}^{3} \langle d_k, d_k \mu_k \rangle \varphi_k'(z_k), \\
&\phi = 2\mathrm{Re} \sum_{k=1}^{3} d_k \varphi_k(z_k), \\
&\langle u, w \rangle = 2\mathrm{Re} \sum_{k=1}^{3} \langle p_k, q_k \rangle \varphi_k(z_k), \\
&v = -2\mathrm{Re}\, a_{55}\mu_4 \varphi_4(z_4),
\end{aligned} \tag{6}$$

where

$$p_k = a_{11}\mu_k^2 + a_{12} + b_{12}\lambda_k, \quad q_k = a_{12}\mu_k + \frac{a_{22} + b_{22}\lambda_k}{\mu_k}, \quad \lambda_k = \frac{(b_{12} + b_{41})\mu_k^2 + b_{22}}{c_{11}\mu_k^2 + c_{22}},$$
$$\mu_4 = \mathrm{i}\sqrt{\frac{a_{33}}{a_{55}}}, \quad d_k = (c_{11}\lambda_k - b_{41})\mu_k, \tag{7}$$

in which, μ_k ($k = 1, 2, 3$) can be determined by solving the following equation:

$$(a_{22} + (2a_{12} + a_{44})\mu^2 + a_{11}\mu^4)(c_{11}\mu^2 + c_{22}) + ((b_{12} + b_{41})\mu^2 + b_{22})^2 = 0. \tag{8}$$

There are three pairs of conjugated plural roots for Eq. (8). And the three roots, whose imaginary parts are positive, are denoted by μ_k ($k = 1, 2, 3$).

At the hole boundary, one has

$$\begin{aligned}
\frac{\mathrm{d}U}{\mathrm{d}x_1} &= -\int_l t_{2s}\,\mathrm{d}s = -\int_l \sigma_{12}\,\mathrm{d}x_2 - \sigma_{22}\,\mathrm{d}x_1,\\
\frac{\mathrm{d}U}{\mathrm{d}x_2} &= \int_l t_{1s}\,\mathrm{d}s = \int_l \sigma_{11}\,\mathrm{d}x_2 - \sigma_{12}\,\mathrm{d}x_1,\\
\varphi_4 &= \int_l \sigma_{23}\,\mathrm{d}x_1 - \sigma_{13}\,\mathrm{d}x_2,\\
\int_l D_n\,\mathrm{d}s &= \int_l D_1\,\mathrm{d}x_2 - D_2\,\mathrm{d}x_1,
\end{aligned} \tag{9}$$

where U is the Airy stress function, and t_{1s} and t_{2s} are the two components of the force on the boundary.

3. Solutions of the problem

Consider the problem of a piezoelectric solid containing an elliptic hole subjected to a uniform stress field σ^∞ and a uniform electric displacement field D^∞ at infinity while the surface of the hole is free of traction and electrically open. The solution may be separated into two parts: one part is the homogeneous solution in which the stress and electric displacement are σ^∞ and D^∞ everywhere; and the other is the "disturbed" state due to the presence of the hole. The second part of the solution should satisfy the boundary conditions of vanishing of both stress and electric displacement at infinity. On the surface of the hole, the stress vanishes after the two parts are superposed. For simplicity, we use the superscript "I" to denote the first part solution, "II" the second part solution, "∞" the quantities at far fields, and "0" the quantities at the surfaces of the hole.

3.1. The stress field for the plate without a hole

Consider an infinite piezoelectric plate subjected to a uniform stress field σ^∞ and a uniform electric displacement field D^∞ at infinity, the solutions are

$$\sigma_{11}^{\mathrm{I}} = \sigma_{11}^\infty, \quad \sigma_{12}^{\mathrm{I}} = \sigma_{12}^\infty, \quad \sigma_{13}^{\mathrm{I}} = \sigma_{13}^\infty, \quad \sigma_{22}^{\mathrm{I}} = \sigma_{22}^\infty, \quad \sigma_{23}^{\mathrm{I}} = \sigma_{23}^\infty, \quad D_1^{\mathrm{I}} = D_1^\infty, \quad D_2^{\mathrm{I}} = D_2^\infty. \tag{10}$$

3.2. The stress field for the plate with an elliptic hole

Since the complex potential $\varphi_k(z_k)$ is a holomorphic function, it can be expressed as follows (Sosa, 1991; Gao and Fan, 1999):

$$\Phi_k[z_k(\varsigma_k)] = \varphi_k(z_k) = \alpha_{k1}\varsigma_k^{-n} \quad (k = 1, 2, 3, 4), \tag{11}$$

where

$$\varsigma_k = \frac{z_k + \sqrt{z_k^2 - (a^2 + \mu_k^2 b^2)}}{a - \mathrm{i}\mu_k b} \quad (k = 1, 2, 3, 4). \tag{12}$$

Because the surface of the hole is free, the following boundary conditions should be met with considering of the relations (9):

$$\begin{aligned}
&2\mathrm{Re}\sum_{k=1}^{3}\Phi_k^{\mathrm{II}}(\sigma) + \left(-\int_L \sigma_{12}^{\mathrm{I}}\,\mathrm{d}x_2 - \sigma_{22}^{\mathrm{I}}\,\mathrm{d}x_1\right) = 0,\\
&2\mathrm{Re}\sum_{k=1}^{3}\mu_k\Phi_k^{\mathrm{II}}(\sigma) + \left(\int_L \sigma_{11}^{\mathrm{I}}\,\mathrm{d}x_2 - \sigma_{12}^{\mathrm{I}}\,\mathrm{d}x_1\right) = 0,\\
&2\mathrm{Re}\sum_{k=1}^{3}\lambda_k\Phi_k^{\mathrm{II}}(\sigma) + \left(-\int_L D_1^{\mathrm{I}}\,\mathrm{d}x_2 - D_2^{\mathrm{I}}\,\mathrm{d}x_1\right) = -\int_L D_n^0\,\mathrm{d}s,\\
&2\mathrm{Re}\ \Phi_4^{\mathrm{II}}(\sigma) + \left(-\int_L \sigma_{13}^{\mathrm{I}}\,\mathrm{d}x_2 - \sigma_{23}^{\mathrm{I}}\,\mathrm{d}x_1\right) = 0.
\end{aligned} \tag{13}$$

Here,

$$\sigma = \mathrm{e}^{\mathrm{i}\theta}, \quad x_1 = a\frac{\sigma + \overline{\sigma}}{2}, \quad x_2 = \mathrm{i}b\frac{\bar{\sigma} - \sigma}{2}. \tag{14}$$

Substituting Eqs. (10) and (11) into Eq. (13) leads to

$$\begin{aligned}
&\alpha_{kn} = 0, \quad (k = 1, 2, 3,\ n \geqslant 2),\\
&\alpha_{k1} = \sum_{j=1}^{3} M_{kj}Q_j, \quad (k = 1, 2, 3),\\
&\alpha_{41} = -\frac{a\sigma_{23}^{\infty} - \mathrm{i}b\sigma_{13}^{\infty}}{2},
\end{aligned} \tag{15}$$

in which

$$M^{-1} = \begin{pmatrix} 1 & 1 & 1 \\ \mu_1 & \mu_2 & \mu_3 \\ \lambda_1 & \lambda_2 & \lambda_3 \end{pmatrix},$$

$$Q = (Q_j) = \begin{pmatrix} -\dfrac{a\sigma_{22}^{\infty} - \mathrm{i}b\sigma_{12}^{\infty}}{2} \\ \dfrac{a\sigma_{12}^{\infty} - \mathrm{i}b\sigma_{11}^{\infty}}{2} \\ -\dfrac{a(D_2^{\infty} - D_2^0) - \mathrm{i}b(D_1^{\infty} - D_1^0)}{2} \end{pmatrix}. \tag{16}$$

The air inside the hole is considered as a homogeneous isotropic linearity medium without polarization and free of electric charge. One has $\nabla \cdot E = 0$. Note that $E = -\nabla\phi$. Thus, $\nabla^2\phi = 0$, where

$$\nabla = \frac{\partial}{\partial x_1}\vec{i} + \frac{\partial}{\partial x_2}\vec{j} + \frac{\partial}{\partial x_3}\vec{k}, \quad \nabla^2 = \frac{\partial^2}{\partial x_1^2} + \frac{\partial^2}{\partial x_2^2} + \frac{\partial^2}{\partial x_3^2}$$

.

For plane problems, the following expression is adopted (Sosa, 1991):

$$\phi^0(x_1, x_2) = -e_1 x_1 - e_2 x_2, \tag{17}$$

where e_1 and e_2 are real constants and

$$E_1^0 = -\frac{\partial \phi^0}{\partial x_1} = e_1, \quad E_2^0 = -\frac{\partial \phi^0}{\partial x_2} = e_2, \quad D_1^0 = \varepsilon_0 E_1^0, \quad D_2^0 = \varepsilon_0 E_2^0. \tag{18}$$

Here, E_1^0, E_2^0, D_1^0, D_2^0 are the electric intensity and electric displacement inside the hole, respectively, and ε_0 is the dielectric constant of the air inside the hole.

There are two constants, e_1, e_2, to be determined in this problem. On the hole surfaces, the electric potential in the media is equal to that inside the hole, namely,

$$\phi^{\mathrm{I}} + \phi^{\mathrm{II}} = \phi^0. \tag{19}$$

Substituting Eqs. (6), (10), (11), (14)–(18) into Eq. (19) and simplifying yield

$$\sigma \bar{h} + h\bar{\sigma} = 0, \tag{20}$$

where

$$\begin{aligned} h &= \sum_{k=1}^{3}[d_k \alpha_{k1}] + \frac{a(E_1^0 - E_1^\infty) + \mathrm{i}b(E_2^0 - E_2^\infty)}{2} \\ &= \frac{a(E_1^0 - E_1^\infty) + \mathrm{i}b(E_2^0 - E_2^\infty)}{2} + \sum_{k=1}^{3}\sum_{i=1}^{2} d_k M_{ki} Q_i - \frac{a(D_2^\infty - D_2^0) - \mathrm{i}b(D_1^\infty - D_1^0)}{2}\sum_{k=1}^{3} d_k M_{k3}. \end{aligned}$$

Analyzing the characteristic of Eq. (20) yields $h_k = 0$ (Gao and Fan, 1999). Thus,

$$\mathrm{Re}\, h = 0, \quad \mathrm{Im}\, h = 0. \tag{21}$$

After considering Eqs. (5) and (18), Eq. (21) can be rewritten in a compact form:

$$\begin{pmatrix} f_{11} & f_{12} \\ f_{21} & f_{22} \end{pmatrix} \begin{pmatrix} D_1^0 \\ D_2^0 \end{pmatrix} = \begin{pmatrix} T_1 \\ T_2 \end{pmatrix}, \tag{22}$$

where

$$\begin{aligned} T_1 &= -d_{\mathrm{R}} + \frac{a}{2}D_2^\infty f_{\mathrm{R}} + \frac{b}{2}D_1^\infty f_{\mathrm{I}} + \frac{a}{2}E_1^\infty, \\ T_2 &= -d_{\mathrm{I}} - \frac{b}{2}D_1^\infty f_{\mathrm{R}} + \frac{a}{2}D_2^\infty f_{\mathrm{I}} + \frac{b}{2}E_2^\infty; \\ d_{\mathrm{R}} &= \mathrm{Re}\sum_{k=1}^{3}\sum_{i=1}^{2} d_k M_{ki} Q_i, \quad d_1 = \mathrm{Im}\sum_{k=1}^{3}\sum_{i=1}^{2} d_k M_{ki} Q_i; \\ f_{\mathrm{R}} &= \mathrm{Re}\sum_{k=1}^{3} d_k M_{k3}, \quad f_1 = \mathrm{Im}\sum_{k=1}^{3} d_k M_{k3}, \\ f_{11} &= \frac{a}{2\varepsilon_0} + \frac{b}{2}f_{\mathrm{I}}, \quad f_{12} = \frac{a}{2}f_{\mathrm{R}}, \\ f_{21} &= -\frac{b}{2}f_{\mathrm{R}}, \quad f_{22} = \frac{b}{2\varepsilon_0} + \frac{a}{2}f_{\mathrm{I}}. \end{aligned} \tag{23}$$

Solving Eq. (22) yields

$$D_1^0 = \frac{f_{22}T_1 - f_{12}T_2}{f_{11}f_{22} - f_{12}f_{21}},$$
$$D_2^0 = \frac{-f_{21}T_1 + f_{11}T_2}{f_{11}f_{22} - f_{12}f_{21}}. \tag{24}$$

Substituting Eqs. (12), (15), (16), (23) and (24) into Eq. (11) yields the complex potential $\varphi_k(z_k)$ ($k = 1, 2, 3, 4$), the solution of the infinite plate with a hole. Then, the "disturbed" stresses can be obtained by using Eq. (6). Sum of the "disturbed" stress and the homogeneous stress provides the final solution of the problem.

4. The case of uni-axial far field mechanical load

Consider the case that the constants μ_k, λ_k ($k = 1, 2, 3$) can be expressed as

$$\mu_1 = \mathrm{i}\mu_0, \quad \mu_2 = \mu_\mathrm{R} + \mathrm{i}\mu_\mathrm{I}, \quad \mu_3 = -\mu_\mathrm{R} + \mathrm{i}\mu_\mathrm{I};$$
$$\lambda_1 = \lambda_0, \quad \lambda_2 = \lambda_\mathrm{R} + \mathrm{i}\lambda_\mathrm{I}, \quad \lambda_3 = \lambda_\mathrm{R} - \mathrm{i}\lambda_\mathrm{I},$$

where $\mu_0 > 0$, $\mu_\mathrm{R} > 0$, $\mu_\mathrm{I} > 0$, λ_0, λ_R, λ_I are real numbers to be determined by Eq. (7). If only the far field mechanical loading in the x_2-direction $\sigma_{22}^{\infty} = \sigma_0$ (MPa) is considered, the expression of the normalized tangential stress $K = \sigma_\theta/\sigma_0$ on the surface of the hole can be obtained by using the following equation:

$$\sigma_\theta = \frac{\sigma_{11}\tan^2\theta + \sigma_{22}t^2 - 2\sigma_{12}t\tan\theta}{t^2 + \tan^2\theta} \quad (0^0 \leqslant \theta < 90^\circ),$$

where $t = b/a$ is the shape factor of the elliptic hole, and

$$\begin{aligned}
K = {} & [1 + t^2 + (-1 + t^2)\cos 2\theta]^2\{\lambda_\mathrm{I}\mu_0\{t^2\sin^2\theta\mu_\mathrm{I}^4 - t^3\cos^2\theta\mu_\mathrm{I}^5 - t\mu_\mathrm{I}^3(\sin^2\theta + 2t^2\cos^2\theta\mu_\mathrm{R}^2) \\
& + \mu_\mathrm{I}(3t\sin^2\theta\mu_\mathrm{R}^2 - t^3\cos^2\theta\mu_\mathrm{R}^4) + t\mu_0^2[t^2\cos^2\theta\mu_\mathrm{I}^3 + t^3\cos^2\theta\mu_\mathrm{I}^4 - t\sin^2\theta\mu_\mathrm{R}^2 + t^3\cos^2\theta\mu_\mathrm{R}^4 + \mu_\mathrm{I}(\sin^2\theta \\
& + t^2\cos^2\theta\mu_\mathrm{R}^2) + t\mu_\mathrm{I}^2(\sin^2\theta + 2t^2\cos^2\theta\mu_\mathrm{R}^2)] + \sin^2\theta\mu_\mathrm{R}^2(t^2\mu_\mathrm{R}^2 - \tan^2\theta) + \sin^2\theta\mu_\mathrm{I}^2(2t^2\mu_\mathrm{R}^2 + \tan^2\theta) \\
& - \mu_0\mu_\mathrm{I}[t^4\cos^2\theta\mu_\mathrm{I}^4 - 2t^2\sin^2\theta\mu_\mathrm{R}^2 + t^4\cos^2\theta\mu_\mathrm{R}^4 + 2t^2\mu_\mathrm{I}^2(\sin^2\theta + t^2\cos^2\theta\mu_\mathrm{R}^2) + \sin^2\theta\tan^2\theta]\} \\
& - \mu_\mathrm{R}\{\sec^2\theta\lambda_0(\sin^2\theta + t^2\cos^2\theta\mu_0^2)(\mu_\mathrm{R}^2 + \mu_\mathrm{I}^2)(\sin^2\theta - 2t\cos^2\theta\mu_\mathrm{I} - t^2\cos^2\theta\mu_\mathrm{I}^2 - t^2\cos^2\theta\mu_\mathrm{R}^2) \\
& + \lambda_\mathrm{R}\mu_0\{t^3\cos^2\theta\mu_\mathrm{I}^4 - t\sin^2\theta\mu_\mathrm{R}^2 + t^3\cos^2\theta\mu_\mathrm{R}^4 + t\mu_0^2(-\sin^2\theta - 2t\sin^2\theta\mu_\mathrm{I} + t^2\cos^2\theta\mu_\mathrm{I}^2 \\
& + t^2\cos^2\theta\mu_\mathrm{R}^2) + \mu_\mathrm{I}^2(3t\sin^2\theta + 2t^3\cos^2\theta\mu_\mathrm{R}^2) - 2\sin^2\theta\mu_\mathrm{I}\tan^2\theta + \mu_0[t^4\cos^2\theta\mu_\mathrm{I}^4 - 2t^2\sin^2\theta\mu_\mathrm{R}^2 \\
& + t^4\cos^2\theta\mu_\mathrm{R}^4 + 2t^2\mu_\mathrm{I}^2(\sin^2\theta + t^2\cos^2\theta\mu_\mathrm{R}^2)\sin^2\theta\tan^2\theta]\}\}\}/\{\{2[1 + t^2 + (-1 + t^2) \\
& \times \cos 2\theta]\sec^2\theta(\sin^2\theta + t^2\cos^2\theta\mu_0^2)[\mu_\mathrm{R}(\lambda_0 - \lambda_\mathrm{R}) + (\mu_0 - \mu_\mathrm{I})\lambda_\mathrm{I}]\}[t^4\cos^4\theta\mu_\mathrm{I}^4 + (\sin^2\theta \\
& - t^2\cos^2\theta\mu_\mathrm{R}^2)^2 + 2t^2\cos^2\theta\mu_\mathrm{I}^2(\sin^2\theta + t^2\cos^2\theta\mu_\mathrm{R}^2)]\}.
\end{aligned} \tag{25}$$

Setting $\theta = 0$ in the above equation yields the expression of the stress concentration factor $K_t = \sigma_\theta|_{\theta=0}/\sigma_0$, namely,

$$\begin{aligned}
K_t = {} & \lambda_\mathrm{I}\frac{-\mu_\mathrm{I}(1 + t\mu_0)(\mu_\mathrm{R}^2 + \mu_\mathrm{I}^2) + \mu_0^2[\mu_\mathrm{I} + t(\mu_\mathrm{R}^2 + \mu_\mathrm{I}^2)]}{t(\mu_\mathrm{R}^2 + \mu_\mathrm{I}^2)\mu_0[\mu_\mathrm{R}(\lambda_0 - \lambda_\mathrm{R}) + (\mu_0 - \mu_\mathrm{I})\lambda_\mathrm{I}]} \\
& - \mu_\mathrm{R}\frac{-\lambda_0\mu_0[2\mu_\mathrm{I} + t(\mu_\mathrm{R}^2 + \mu_\mathrm{I}^2)] + \lambda_\mathrm{R}[\mu_0^2 + (1 + t\mu_0)(\mu_\mathrm{R}^2 + \mu_\mathrm{I}^2)]}{t(\mu_\mathrm{R}^2 + \mu_\mathrm{I}^2)\mu_0[\mu_\mathrm{R}(\lambda_0 - \lambda_\mathrm{R}) + (\mu_0 - \mu_\mathrm{I})\lambda_\mathrm{I}]}.
\end{aligned} \tag{26}$$

From Eq. (26), it can be readily proved that the following equation is valid:

$$K_t = 1 + \frac{K_t|_{t=1} - 1}{t}, \tag{27}$$

where $K_t|_{t=1}$ is the stress concentration factor of a circular hole ($t = 1$), and

$$\begin{aligned} K_t|_{t=1} = {} & \lambda_{\mathrm{I}} \frac{-\mu_{\mathrm{I}}(1+\mu_0)(\mu_{\mathrm{R}}^2+\mu_{\mathrm{I}}^2) + \mu_0^2[\mu_{\mathrm{I}} + (\mu_{\mathrm{R}}^2+\mu_{\mathrm{I}}^2)]}{(\mu_{\mathrm{R}}^2+\mu_{\mathrm{I}}^2)\mu_0[\mu_{\mathrm{R}}(\lambda_0-\lambda_{\mathrm{R}}) + (\mu_0-\mu_{\mathrm{I}})\lambda_{\mathrm{I}}]} \\ & - \mu_{\mathrm{R}} \frac{-\lambda_0\mu_0[2\mu_{\mathrm{I}} + (\mu_{\mathrm{R}}^2+\mu_{\mathrm{I}}^2)] + \lambda_{\mathrm{R}}[\mu_0^2 + (1+\mu_0)(\mu_{\mathrm{R}}^2+\mu_{\mathrm{I}}^2)]}{(\mu_{\mathrm{R}}^2+\mu_{\mathrm{I}}^2)\mu_0[\mu_{\mathrm{R}}(\lambda_0-\lambda_{\mathrm{R}}) + (\mu_0-\mu_{\mathrm{I}})\lambda_{\mathrm{I}}]}. \end{aligned} \tag{28}$$

The derived formula is applied to a transversely isotropic piezoelectric material, PZT-4, for validating its correctness. The following data from Sosa (1991) are used:

$$\begin{aligned} & a_{11} = 8.205 \times 10^{-12}, \quad a_{12} = -3.144 \times 10^{-12}, \\ & a_{22} = 7.495 \times 10^{-12}, \quad a_{44} = 19.3 \times 10^{-12}\ (\mathrm{m^2\ N^{-1}}); \\ & b_{12} = -16.62 \times 10^{-3}, \quad b_{22} = 23.96 \times 10^{-3}, \\ & b_{41} = 39.4 \times 10^{-3}\ (\mathrm{m^2\ C^{-1}}); \\ & c_{11} = 7.66 \times 10^{7}, \quad c_{22} = 9.82 \times 10^{7}\ (\mathrm{V^2\ N^{-1}}). \end{aligned} \tag{29}$$

Inserting these constants into Eq. (8) yields

$$\begin{aligned} & \mu_1 = 1.2184867\mathrm{i}, \\ & \mu_2 = 0.20060870 + 1.0698790\mathrm{i}, \\ & \mu_3 = -0.20060708 + 1.0698790\mathrm{i}. \end{aligned} \tag{30}$$

The dielectric constant of air is $\varepsilon_0 = 8.854 \times 10^{-12}$. For demonstrations, the elastic material constants for the transversely isotropic material are set to be the same as that of the piezoelectric material. Concrete results for the stress concentration factors of the isotropic elastic material, the transversely isotropic elastic material and the transversely isotropic piezoelectric material are listed in Table 1. Based on these data, the following expressions can be obtained:

(1) for the isotropic material

$$K_t = 1 + \frac{K_t|_{t=1} - 1}{t} = 1 + \frac{2}{t};$$

(2) for the transversely isotropic material

$$K_t = 1 + \frac{K_t|_{t=1} - 1}{t} = 1 + \frac{1.9567}{t};$$

(3) for the PZT-4

$$K_t = 1 + \frac{K_t|_{t=1} - 1}{t} = 1 + \frac{1.7215}{t}.$$

It should be pointed out that the Eqs. (26) and (28) are only valid for the transversely isotropic piezoelectric material since the eigenvalue μ_k ($k = 1, 2, 3$) is solved from the eigenequation (8), closely related to the values of the particular material constants. Thus, it is proved that Eq. (27) is also valid for both isotropic materials and transversely isotropic materials. It may be conjectured that, for any elastic or piezoelectric materials, Eq. (27) may be valid.

Table 1
Comparisons on the stress concentration factor of the present solutions, transversely isotropic elastic solutions and isotropic elastic solutions

The hole shape factors $t = \frac{b}{a}$	The isotropic elastic solutions K_{t1}	The transversely isotropic elastic solutions		The transversely isotropic piezoelectric solutions		
		K_{t2}	Relative changes $\frac{K_{t1}-K_{t2}}{K_{t1}}$ (%)	K_{t3}	Relative changes $\frac{K_{t1}-K_{t3}}{K_{t1}}$ (%)	Relative changes $\frac{K_{t2}-K_{t3}}{K_{t2}}$ (%)
0.01	201	196.6700	2.1542	173.3110	13.7756	11.8773
0.02	101	98.8350	2.1436	87.1173	13.7452	11.8558
0.03	67.6667	66.2234	2.1330	58.4026	13.6908	11.8097
0.05	41	40.1340	2.1122	35.4371	13.5680	11.7030
0.07	29.5714	28.9529	2.0915	25.5966	13.4414	11.5923
0.08	26	25.4588	2.0815	22.5216	13.3785	11.5371
0.1	21	20.5670	2.0619	18.2169	13.2529	11.4266
0.2	11	10.7835	1.9682	9.6080	12.6544	10.9007
0.3	7.6667	7.5223	1.8826	6.7386	12.1055	10.4191
0.4	6	5.8918	1.8042	5.3039	11.6017	9.9775
0.5	5	4.9134	1.7320	4.4431	11.1380	9.5718
0.6	4.3333	4.2612	1.6652	3.8692	10.7098	9.1977
0.7	3.8571	3.7953	1.6035	3.4594	10.3131	8.8515
0.8	3.5	3.4459	1.5463	3.1519	9.9451	8.5308
0.9	3.2222	3.1741	1.4931	2.9128	9.6021	8.2319
1	3	2.9567	1.4433	2.7215	9.2820	7.9535

4.1. Stress distributions

The variations of the normalized stress $K = \sigma_\theta/\sigma_0$ with the angle in the vicinity of the hole and the stress concentration factor $K_t = \sigma_\theta|_{\theta=0}/\sigma_0$ with the shape factor of the hole $t = b/a$ are considered with emphasis placed on the comparison of the solutions of isotropic elastic materials, transverse isotropic elastic materials and transverse isotropic piezoelectric materials. Fig. 1 shows the variation of the normalized stress $K = \sigma_\theta/\sigma_0$ along the surface of the hole. Curves of isotropic and transversely isotropic elastic plates almost coincide with each other, while the curve of the transversely isotropic piezoelectricity obviously deviates from them. At the locations with the highest stress concentration ($\theta = 0$ and π), the stress in the piezoelectricity is about 8.0% and 11.4% lower than that in the elasticity for $t = 1$ and 0.1, respectively. It is also found that the present results are in excellent coincidence with the related results of Sosa (1991), Deng and Wang (2002), and Dai and Guo (2004) when $t = 1$.

A comprehensive comparison of the stress concentrations at the elliptic hole in the piezoelectric and elastic plates is presented in Fig. 2 and Table 1. From Table 1, it can be found that the difference of the three solutions increases slowly as the hole degenerating into a crack. The piezoelectric-mechanical coupling in the PZT-4 can alleviate the stress concentration for about 8% for circular holes and up to 12% when t decreases to 0.01. Due to the electromechanical coupling effect, however, the stress concentration factor in a transverse isotropic piezoelectric material is obviously weaker when the materials are polarizing along the z-axis. Therefore, the electromechanical coupling effect is helpful for the safety of materials and structures.

Then, the distribution of the normalized stress $X_{t\sigma} = \sigma_\theta/\sigma_\theta^0$ on the section at $\theta = 0$ is studied. Fig. 3(a)–(c) show that, whenever the value of the hole shape factor t is, the curves for the isotropic and transversely isotropic elastic bodies are nearly coincident, while the curve of the transversely isotropic piezoelectricity is obviously higher as the σ_θ^0 in the piezoelectricity is lower. The difference between the normalized stress $X_{t\sigma} = \sigma_\theta/\sigma_\theta^0$ of the piezoelectricity and that of the elasticity reaches 7.17%, 11.37% and 11.96% at $x = 3$ on the section for $t = 1$, 0.1 and 0.01, respectively.

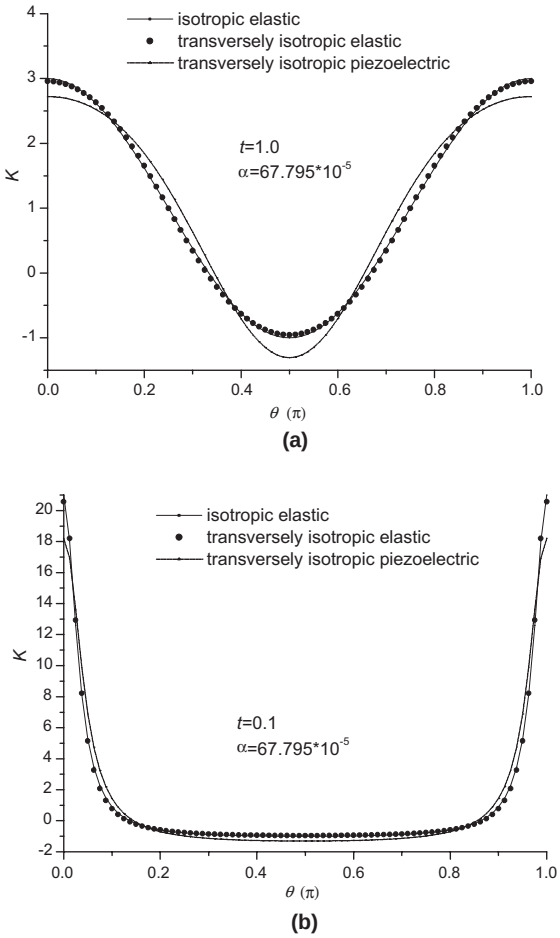

Fig. 1. Variations of the normalized stress $K = \sigma_\theta/\sigma_0$ with θ along the edge of a hole in infinite sheets subjected to remote tensile loading. (a) $t = 1$; (b) $t = 0.1$.

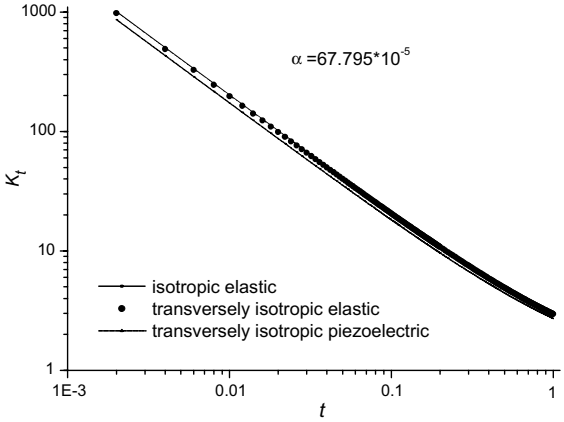

Fig. 2. Variations of the stress concentration factor $K_t = \sigma_\theta|_{\theta=0}/\sigma_0$ at the root of the elliptic hole with the shape factor t of the hole.

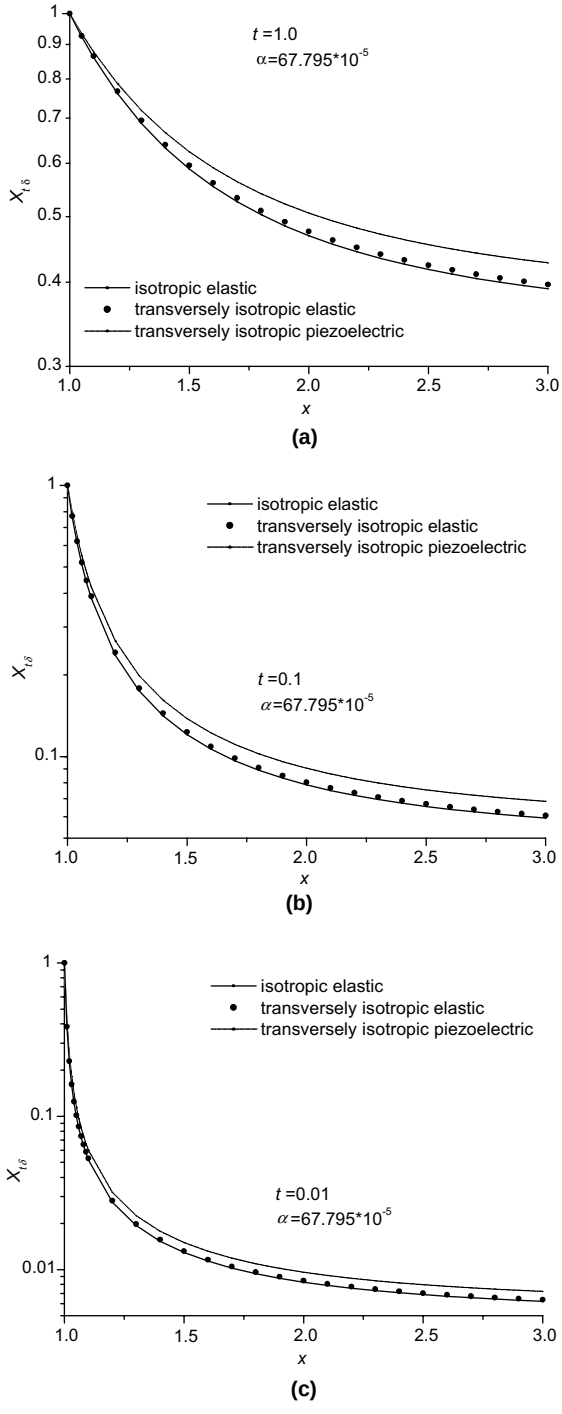

Fig. 3. Distributions of the normalized stress $X_{t\sigma} = \sigma_\theta/\sigma_\theta^0$ on the section at $\theta = 0$ for different the shape factors of the holes. (a) $t = 1$; (b) $t = 0.1$; (c) $t = 0.01$.

Fig. 4 shows the variation of the normalized electric displacement $K_{d\sigma} = (D_\theta|_{\theta=0}/\sigma_0) \times 10^8$ and the normalized electric field $K_{e\sigma} = -(E_\theta|_{\theta=0}/\sigma_0) \times 10^2$. It is interesting to see that the variation of $K_{d\sigma}$ is nearly linear to t in the log–log coordinates. $K_{e\sigma}$ is approximately linear to t for smaller t (say $t < 0.1$), while becomes nonlinear for $t > 0.1$ in the same coordinates. It should be noted that, an amplification factor of 8 orders is applied to $K_{d\sigma}$ while the factor to $K_{e\sigma}$ is only 2 powers of ten in the figure. As the coefficient factors of the electric displacements are about 8 order higher than that of the stresses in Eq. (4), so the contribution of the piezoelectric effect to the strain field near the hole can reach the same order as the mechanical stresses. This is the reason why the piezoelectric effect can release the stress concentration at the hole.

4.2. The effect of the dielectric parameter α

The electric conductive condition of the medium in the hole is always an important issue in practical applications. In this section the influence of the dielectric parameter α of the medium inside the hole on

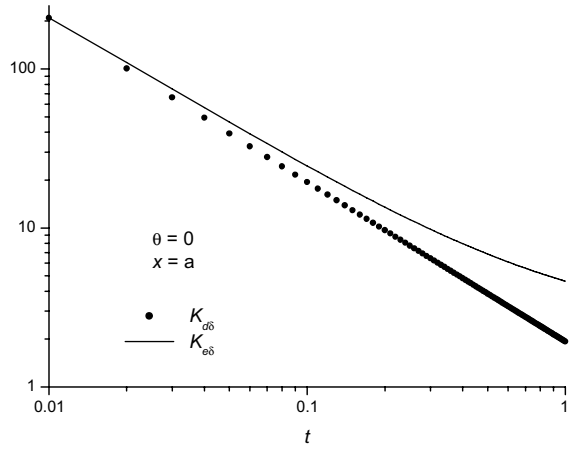

Fig. 4. Variations of the concentration factors of the electric displacement $K_{d\sigma} = (D_\theta|_{\theta=0}/\sigma_0) \times 10^8$ and the electric field $K_{e\sigma} = (E_\theta|_{\theta=0}/\sigma_0) \times 10^2$ at the root of the elliptic hole with the shape factor t of the hole.

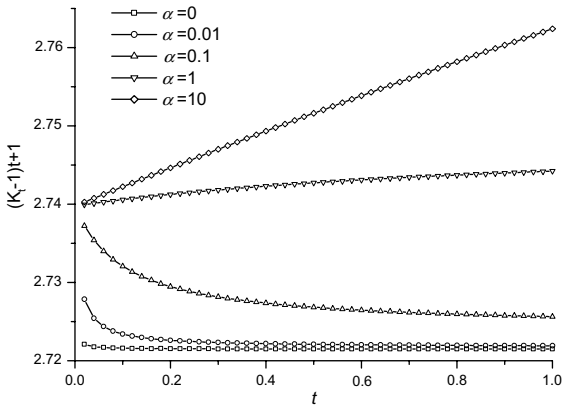

Fig. 5. Variations of the concerned stress concentration factor $K_t|_{t=1} = (K_t - 1)t + 1$ at the root of the elliptic hole with the shape factor t of the hole for different values of parameter-α.

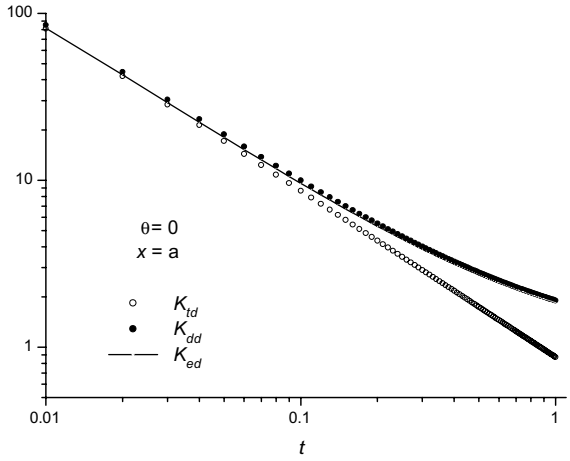

Fig. 6. Variations of the concentration factors of the stress $K_{t\mathrm{d}} = (\sigma_\theta|_{\theta=0}/D_0) \times 10^{-8}$, the electric displacement $K_{\mathrm{dd}} = D_\theta|_{\theta=0}/D_0$ and the electric field $K_{\mathrm{ed}} = (E_\theta|_{\theta=0}/D_0) \times 10^{-8}$ at the root of the elliptic hole with the shape factor t of the hole.

the concerned stress concentration factor $K_t|_{t=1} = (K_t - 1)t + 1$ will be analyzed in details. Fig. 5 shows the influence of α on the stress concentration parameter $K_t|_{t=1}$ at the root of the hole for various shape factor t. It is found that the maximal difference in stress concentration factor caused by the change of α from 0 to 10 is less than 1.5% at $t = 1$. Furthermore, the variation of $K_t|_{t=1}$ with the shape factor t is within 0.82% in all the cases and nearly disappears when $\alpha = 0$. This means that the important relation (27) can hold good for any electric boundary condition in the hole in piezoelectric materials, or the stress concentration factor K_t is in inverse proportion to the shape factor t of the hole in both elastic and piezoelectric bodies.

5. The case of uni-axial far field electric displacement load

In this section, solutions under the far field electric displacement $D_2^\infty = D_0$ loading will be discussed. The concentration factors of the stress $K_{t\mathrm{d}} = (\sigma_\theta|_{\theta=0}/D_0) \times 10^{-8}$, the electric displacement $K_{\mathrm{dd}} = D_\theta|_{\theta=0}/D_0$ and the electric filed $K_{\mathrm{ed}} = (E_\theta|_{\theta=0}/D_0) \times 10^{-8}$ in the vicinity of elliptic holes in the piezoelectric material are plotted in Fig. 6. It can be seen that the curves of K_{dd} is nearly linear to t in the log–log coordinates. The curves of $K_{\mathrm{e}\sigma}$ and $K_{t\mathrm{d}}$ are nearly coincident with each other and nearly linear to t for $t < 0.1$, and become nonlinear for larger t in the log–log coordinates. Obviously, the concentrations of stress, electric displacement and electric filed are significant even under the pure far field electric displacement loading. Therefore, the fracture problem induced by electric loading can be crucial in piezoelectric structures and instruments.

6. Conclusions

The two-dimensional plane strain problems of both elastic and transversely isotropic piezoelectric materials containing an elliptic hole subjected to a uniform far field stress and far field electric displacement are solved analytically using the complex variables theory. The effects of electric boundary condition and electric conduction property of the medium in the hole are discussed in details. The solution of the normalized stress $K = \sigma_\theta/\sigma_0$ is obtained explicitly on the surface of the hole and on the section along the axle of the elliptic hole. A concise relationship between the stress concentration factor of an elliptic hole with aspect

shape ratio t and that of a circular hole with $t = 1$ is obtained as $K_t = 1 + \frac{K_t|_{t=1}-1}{t}$, which is prove to be valid for both elastic materials and piezoelectric materials under any electric boundary condition. The influence of the electromechanical coupling effect and the dielectric parameter of the air inside the hole on the stress distribution and on the concerned stress concentration factor has been studied in details. It is shown that the electromechanical coupling effect is helpful to reduce the stress concentration at holes. The influence of elastic transversely isotropic property on the stress concentration factor in elastic materials is very weak. However, obvious difference of stress σ_θ between the piezoelectric material and the two elastic materials is observed. Results also show that the influence of the dielectric parameter of the air inside the hole on the stress distributions on the section at $\theta = 0$ and on the concerned stress concentration factor on the surface of the hole is within 1.5% in a wide range of the dielectric parameter. Distributions of the mechanical and electrical components at the rim of the hole or along the x-axis are obtained for the elliptic holes. It is also shown that significant stress, electric displacement and electric field concentrations can be caused by uniform far field electric displacement loading. The present results are verified by comparing with available existing data.

Acknowledgements

This work is supported by the National Natural Science Foundation of China (Nos. 50275073 and 10372044) and the Aeronautic Science Foundation of China (No. 03B52011). We thank Professor Wei-Xun Fan, Pu-Hui Chen for helpful discussions.

References

Chung, M.Y., Ting, T.C.T., 1996. Piezoelectric solid with an elliptic inclusion or hole. Int. J. Solids Struct. 33, 3343–3361.

Dai, L., Guo, W., 2004. On the problem of piezoelectric solid with an elliptic hole. Acta Mech. Sinica 36, 224–228 (in Chinese).

Deng, Q., Wang, T., 2002. Study on an infinite piezoelectric solid with elliptic notch. Acta Mech. Sinica 34, 109–115 (in Chinese).

Gao, C., Fan, W., 1999. Exact solutions for the plane problem in piezoelectric materials with an elliptic or a crack. Int. J. Solids Struct. 36, 2527–2540.

Hao, T., Shen, Z., 1994. A new electric boundary condition of electric fracture mechanics and its applications. Eng. Fract. Mech. 47, 793–802.

Pak, Y.E., 1990. Crack extension force in a piezoelectric material. ASME J. Appl. Mech. 57, 647–653.

Pak, Y.E., 1992. Linear electroelastic fracture mechanics of piezoelectric materials. Int. J. Fract. 29, 2613–2622.

Sosa, H., 1991. Plane problems in piezoelectric media with defects. Int. J. Solids Struct. 28, 491–505.

Sosa, H., 1992. On the fracture mechanics of piezoelectric solids. Int. J. Solids Struct. 29, 2613–2622.

Sosa, H., Khutoryansky, N., 1996. New developments concerning piezoelectric materials with defects. Int. J. Solids Struct. 33, 3399–3414.

Sosa, H., Pak, Y., 1990. Three-dimensional eigenfunction analysis of a crack in a piezoelectric material. Int. J. Solids Struct. 26, 1–15.

Suo, Z. et al., 1992. Fracture mechanics for piezoelectric ceramics. J. Mech. Phys. Solids 40, 739–765.

Ting, T.C.T., Yan, G., 1991. The anisotropic elastic hole or rigid inclusion. Int. J. Solids Struct. 27, 1879–1894.

Wang, X., Shen, Y., 2002. Exact solution for mixed boundary value problems at anisotropic piezoelectric bimaterial interface and unification of various interface defects. Int. J. Solids Struct. 39, 1591–1619.

Wang, X., Zhou, Y., Zhou, W., 2004. A novel hybrid finite element with a hole analysis of plane piezoelectric medium with defects. Int. J. Solids Struct. 41, 7111–7128.

Zhang, T., Tong, P., 1996. Fracture mechanics for a mode III crack in a piezoelectric material. Int. J. Solids Struct. 33, 343–359.

Zhang, T., Qian, C., Pin, T., 1998. Linear electro-elastic analysis of a cavity or a crack in a piezoelectric material. Int. J. Solids Struct. 35, 2121–2149.

Zhou, Y., Wang, X., 2004. Analyses of crack-tip fields of plane piezoelectric materials by the hybrid stress finite element method. Acta Mech. Sinica 36, 354–358 (in Chinese).